

Electronic Supplementary Information

Exploring the fluorescence enhancement of split G-quadruplex towards DNA-templated AgNCs and its application in omethoate detection

Li Yin, ‡^a Hui Zhang, ‡^a Ying Wang, ^a Liang He ^{*b} and Lihua Lu ^{*a}

^a College of Chemistry and Pharmaceutical Sciences, Qingdao Agricultural University, Qingdao 266109, China

^b Penglai Jiaxin Dye Chemical., LTD., Yantai 265600, China

*Corresponding author. E-mail: lulihua2012@qau.edu.cn (L. Lu)

Tel: +86 532 58957895.

E-mail: hel@jiaxinchemic.com (L. He).

‡These authors contributed equally to this work.

Experimental section

Chemicals and Materials

OME was bought from Youhong Biochemical Technology Co., Ltd. Other chemicals were bought from Sinopharm Chemical Reagent Co., Ltd. (Shanghai China). The oligonucleotides used in this work were provided by Shanghai Sangon Biotech Co. (Shanghai, China), which were presented in Table S1.

Preparation of the DNA-templated AgNCs

Firstly, DNA-templated strand MAg (100 μM , 20 μL) was added into phosphate buffer (PB, 20 mM, pH = 7.0, 156 μL). Then, freshly prepared AgNO_3 aqueous solution (1000 μM , 12 μL) was added, and the mixture was shaken vigorously on a vortex for 1 min. Afterwards, the reactant was placed in a refrigerator to react in the dark at 4 $^\circ\text{C}$ for 30 min¹. Then, the freshly prepared NaBH_4 solution (1000 μM , 12 μL) was added in the mixture, and the mixture was vortexed vigorously for 1 min. Finally, the reactant was placed in a refrigerator and incubated at 4 $^\circ\text{C}$ in the dark for 2 h. The final concentrations of MAg, AgNO_3 , and NaBH_4 were 10 μM , 60 μM , and 60 μM , respectively (molar ratio 1 : 6 : 6)².

The formation of three-element split G4 structure

The six split modes of G4 are 1:11, 2:10, 3:9, 4:8, 5:7 and 6:6, respectively³. Taking the split mode of 6:6 as an example, the AgNCs template-contained DNA strand MAg (10 μM , 10 μL) was incubated with L_6 (100 μM , 1 μL) and R_6 (100 μM , 1 μL) at 37 $^\circ\text{C}$ for 1 h, and then KNO_3 solution (1000 mM, 10 μL) and 78 μL of 20 mM PB (20 mM, pH = 7.0) were added into the mixture to promote the formation of G4. After the reactant was incubated at 37 $^\circ\text{C}$ for 2 h with light-free, the emission spectra of the samples were recorded at the excitation wavelength of $\lambda_{\text{ex}} = 520$ nm. The operation steps for other split methods were similar to this one.

Fluorescent assay of OME

The aptamer chain AP2 (100 μ M, 2 μ L) was firstly incubated with 5 μ L different concentrations of OME at 37 $^{\circ}$ C for 40 min to promote the full binding of OME to its aptamer⁴. Then, DNA template MPAG (10 μ M, 20 μ L) and L₆ (100 μ M, 2 μ L) were added and incubated at 37 $^{\circ}$ C for 1 h to promote the combination of the three DNA strands. Then KNO₃ solution (1000 mM, 20 μ L) was added, the system was filled to 200 μ L with PB (20 mM, pH = 7.0), and the mixture was incubated at 37 $^{\circ}$ C for 2 h with light-free to facilitate the formation of G4. Then, freshly prepared AgNO₃ aqueous solution (1000 μ M, 12 μ L) and the freshly prepared NaBH₄ solution (1000 μ M, 12 μ L) was added in the mixture, and the mixture was vortexed vigorously for 1 min. Finally, the reactant was placed in a refrigerator and incubated at 4 $^{\circ}$ C in the dark for 2 h. The emission spectra of the samples at the excitation wavelength $\lambda_{\text{ex}} = 520$ nm were tested. The relative fluorescent intensity is used to evaluate the detection signal, which is presented as $I_0 - I$, where I_0 means the fluorescent intensity of the detection system without OME at $\lambda_{\text{em}} = 580$ nm, while I presents the fluorescent intensity in the presence of OME at $\lambda_{\text{em}} = 580$ nm.

Optimization experiments

In the optimization experiment, the prepared samples were divided into two groups. The initial fluorescence intensity of AgNCs is recorded as " I_0 ", the fluorescence intensity after the formation of split G4 was denoted as " I ", and the relative intensity " $I - I_0$ " was used to assess the effect of each factor on the experiment.

When optimizing pH, the ratio of MPAG, AgNO₃, NaBH₄ was 1:6:6, K⁺ concentration was 100 mM, and PB buffer solutions of different pH (6.0, 6.5, 7.0, 7.5, 8.0) were added. The interaction time was 2 h. The other experimental steps were the same as that the steps in the formation of three-element split G4 structure. The whole reaction process is protected from light.

When optimizing the ratio of DNA template, AgNO₃, and NaBH₄, different ratios of them were used in the experiments, which were 1:3:3, 1:6:6, 1:12:12, 1:18:18 and

1:36:12, respectively. The concentration of MAg was fixed as 1 μ M, and the concentrations of AgNO₃ and NaBH₄ were changed according to the above ratios. The pH was 7.0, and K⁺ concentration was 100 mM. The interaction time between G4 with DNA-AgNCs was 2 h.

When optimizing the concentration of K⁺, the ratio of DNA template, AgNO₃, NaBH₄ was 1:6:6, and the solution pH was 7.0. the incubation time was 2 h. Different concentrations of K⁺ (10, 20, 50, 80, 100 and 120 mM) were added. The following steps were the same as that the steps in the formation of three-element split G4 structure.

When optimizing the interaction time between split G4 with DNA-AgNCs, the ratio of DNA template, AgNO₃, NaBH₄ was 1:6:6. The solution pH was 7.0, and the concentration of K⁺ was 100 mM. Different incubation time (5, 10, 20, 40, 60, 90, 120 and 150 min) were used to incubate split G4 with DNA-AgNCs. Then, the following steps were the same as that the steps in the formation of three-element split G4 structure.

Gel electrophoresis experiments

The electrophoresis method selected in the experiment was polyacrylamide gel electrophoresis. 30% polyacrylamide hydrogel, 5 \times TBE buffer, tetramethylethylenediamine (TEMED) and 10% ammonium persulfate solution (APS) were used in this experiment. After the samples were prepared, the acrylamide gel was reacted in 1 \times TBE buffer at 110 V for 45 min, and the gel was stained with gel-red at 37 $^{\circ}$ C for 30 min. Finally, the Gel Doc XR+ imaging system was used for imaging and photography.

Circular dichroism (CD) measurements

CD spectra of the L_x/R_y/MAg systems were measured on a spectropolarimeter (Applied Photophysics, London, UK) in 1 mm pathlength cuvettes at room temperature. The six split modes of G4 were investigated to prove the formation of G-

quadruplex conformation. Taking the split mode of 6:6 as an example, the MAg (100 μM , 4 μL) was incubated with L_6 (100 μM , 4 μL) and R_6 (100 μM , 4 μL) at 37 $^\circ\text{C}$ for 1 h, and then metal ions solution (KCl or LiCl, 1000 mM, 20 μL) and 168 μL of PB buffer (20 mM, pH = 7.0) were added into the mixture to promote the formation of G4. For comparison, the $\text{L}_x/\text{R}_y/\text{MAg}$ system was incubated without K^+ or Li^+ solution added, that were also investigated. The final concentration of MAg, L_6 , R_6 , metal ions (K^+ or Li^+) were 2 μM , 2 μM , 2 μM , 100 mM, respectively. After the mixture was incubated at 37 $^\circ\text{C}$ for 2 h, the CD spectra was recorded in the range from 220 nm to 320 nm.

Selective and Interfering Experiments

Eight commonly used pesticides were selected to demonstrate the selectivity of the detection platform, including omethoate, phorate, profenofos, amphophos, malathion, metalaxyl, phoxim, oxyphosphorus. When the interference of this assay platform was investigated, the concentration of OME was 200 nM, and the other eight pesticides were all at 1 μM . The specific steps of the experiment were the same as the detection of OME in buffer solution.

Real sample preparation

The cabbage samples, apple samples and school tap water were selected as actual samples to analyze and detect OME. The cabbage sample was first crushed. Then, 5 g of the sample and 25 mL of methanol were added to the beaker, and the mixture was vigorously stirred for 6 hours at room temperature. After that, the mixture was centrifuged at 13,000 rpm for 15 min, and the supernatant was filtered for use. 5 g of apples with peels were taken, chopped, and added with 10 mL of acetonitrile and 2.5 mL of water. The mixture was vigorously stirred at room temperature for 10 min, then sonicated for 30 min and filtered. The filtrate was concentrated by rotary evaporation at 65 $^\circ\text{C}$. Finally, the sample was furtherly filtrated by 0.22 μM membrane filtration.

Table S1 DNA sequences used in this detection platform.

Name	Sequence (5'-3')
L ₁	<u>G</u> ATCATAGTC
L ₂	<u>G</u> ₂ ATCATAGTC
L ₃	<u>TG</u> ₃ ATCATAGTC
L ₄	<u>GTG</u> ₃ ATCATAGTC
L ₅	<u>G₂TG</u> ₃ ATCATAGTC
L ₆	<u>TG₃TG</u> ₃ ATCATAGTC
R ₁₁	GTCGT ₂ CGA <u>TG₃TG₃TG₃TG₂</u>
R ₁₀	GTCGT ₂ CGA <u>TG₃TG₃TG₃TG</u>
R ₉	GTCGT ₂ CGA <u>TG₃TG₃TG₃</u>
R ₈	GTCGT ₂ CGA <u>TG₃TG₃TG₂</u>
R ₇	GTCGT ₂ CGA <u>TG₃TG₃TG</u>
R ₆	GTCGT ₂ CGA <u>TG₃TG₃</u>
L ₆₋₁	<u>TG₃TG₃</u> (T)ATCATAGTC
L ₆₋₂	<u>TG₃TG₃</u> (T ₂)ATCATAGTC
L ₆₋₃	<u>TG₃TG₃</u> (T ₃)ATCATAGTC
R ₆₋₁	GTCGT ₂ CGA(T) <u>TG₃TG₃</u>
R ₆₋₂	GTCGT ₂ CGA(T ₂) <u>TG₃TG₃</u>
R ₆₋₃	GTCGT ₂ CGA(T ₃) <u>TG₃TG₃</u>
MAg	<i>GACTATGATC₃T₂A₂TC₃CTCGA₂CGAC</i>
AP2	AGCT₂GCTGCAGCGAT₂CT₂GATCGC₂ACAGAGCT <u>TG₃TG₃</u>
MPAg	GACTATGATC ₃ T ₂ A ₂ TC ₃ CAG(CT) ₂ GTG ₂ CGA

^a The underlined and italic bases is the G4 sequences. The bold bases are aptamer sequence of OME. The italic bases are the template of AgNCs. T bases in brackets from L₆₋₁ to R₆₋₃ decide spacer length.

Table S2 Comparison with other methods in the OME detections.

Methods	Detection limit	Linear range	Reference
Exploring the fluorescence enhancement of split G-quadruplex towards DNA-templated AgNCs and its application in omethoate detection	4.16 nM	5–200 nM	This method
Aptamer-wrapped gold nanoparticles for the colorimetric detection of omethoate	0.1 μM	0.1–10 μM	5
Sulphur-doped graphene quantum dot based fluorescent turn-on aptasensor for selective and ultrasensitive detection of	4.7 nM	4.7–470 μM	6

omethoate			
Quantum dot-DNA aptamer conjugates coupled with capillary electrophoresis: A universal strategy for ratiometric detection of organophosphorus pesticides	0.23 μM	0.7–10.0 μM	7
Multi-branch chemiluminescence–molecular imprinting sensor for sequential determination of carbofuran and omethoate in foodstuff	0.20 μM	0.469–42.22 μM	8
Multicolor colorimetric sensor for detection of omethoate based on the inhibition of the enzyme-induced metallization of gold nanorods	0.39 nM	0.28 –28.14 μM	9
Organophosphorus pesticides detection using broad-specific single-stranded DNA based fluorescence polarization aptamer assay	23.4 nM	23.45 nM–46.91 μM	10
Development of a single aptamer-based surface enhanced Raman scattering method for rapid detection of multiple pesticides	24 μM	4.8–48 μM	11
A gold-based nanobeacon probe for fluorescence sensing of organophosphorus pesticides	2.35 μM	27 pM–27 μM	12
Novel fluorescence sensor based on all-inorganic perovskite quantum dots coated with molecularly imprinted polymers for highly selective and sensitive detection of omethoate	0.088 μM	0.23–1.88 μM	13
Porous hierarchical peony-like cobalt-based bimetallic oxides structured by ultrathin nanosheets for highly sensitive electrochemical pesticides detection	0.033 pM	0.469 pM–469 nM	14
A colorimetric paper sensor based on the domino reaction of acetylcholinesterase and degradable $\gamma\text{-MnOOH}$ nanozyme for sensitive detection of organophosphorus pesticides	1.64 nM	0.23–2.35 μM	15
Single-atom Ce-N-C nanozyme bioactive paper with a 3D-printed platform for rapid detection of organophosphorus and carbamate pesticide residues	2.62 μM	0.47–3.28 mM	16
Gas chromatography with flame photometric detection of 31 organophosphorus pesticide residues in <i>Alpinia oxyphylla</i> dried fruits	9.38 nM	28.14 nM–4.69 μM	17
Determination of eight selected organophosphorus insecticides in postmortem blood samples using solid-phase extraction and gas	0.47 μM	0.47–1.17 μM	18

chromatography/mass spectrometry			
Label-free homogeneous electroanalytical platform for pesticide detection based on acetylcholinesterase-mediated DNA conformational switch integrated with rolling circle amplification	9.85 nM	0.047–46.91 μ M	19
Method for determination of acephate, methamidophos, omethoate, dimethoate, ethylenethiourea and propylenethiourea in human urine using high-performance liquid chromatography-atmospheric pressure chemical ionization tandem mass spectrometry	6.00 nM	1.50–54.60 nM	20
A zero-background fluorescent aptasensor for ultrasensitive detection of pesticides based on magnetic three-dimensional DNA walker and poly(T)-templated copper nanoparticles	0.22 nM	0–200 nM	21

Table S3 Determination of OME in apple and tap water samples.

Sample No.	Add omethoate (nM)	Detected omethoate (nM)	SD (n=5)	Recovery (%)
Apple 1	50	49.2	4.5	98.4
Apple 2	100	100.6	3.2	100.6
Apple 3	200	198.8	2.7	99.4
Tap water 1	50	51.1	5.2	102.2
Tap water 2	100	99.1	2.3	99.1
Tap water 3	200	201.5	1.8	100.7

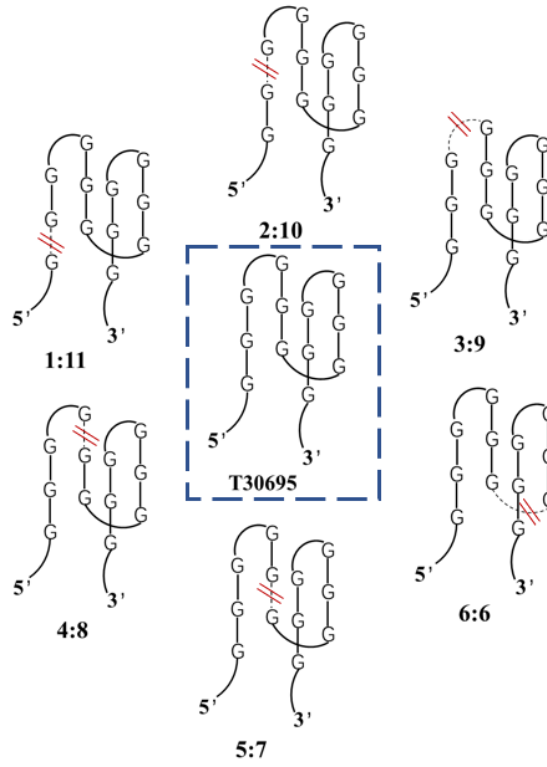


Fig. S1 Split mode diagram of G4.

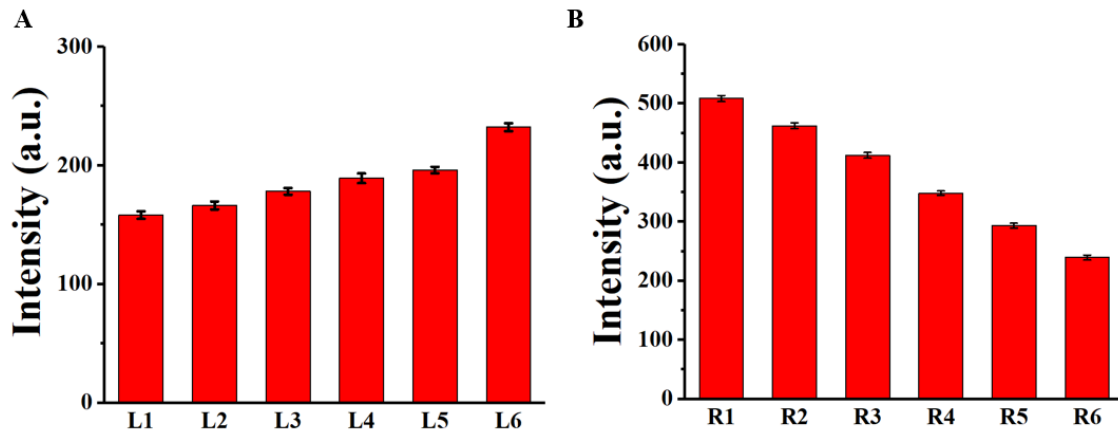


Fig. S2 The luminescence enhancement of AgNCs by (A) left arms and (B) right arms.

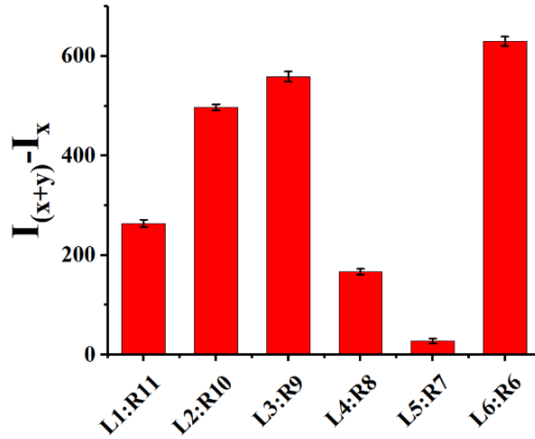


Fig. S3 The fluorescence enhancement of three-element system $L_x/R_y/AgNCs$ relative to two-element system of $L_x/AgNCs$.

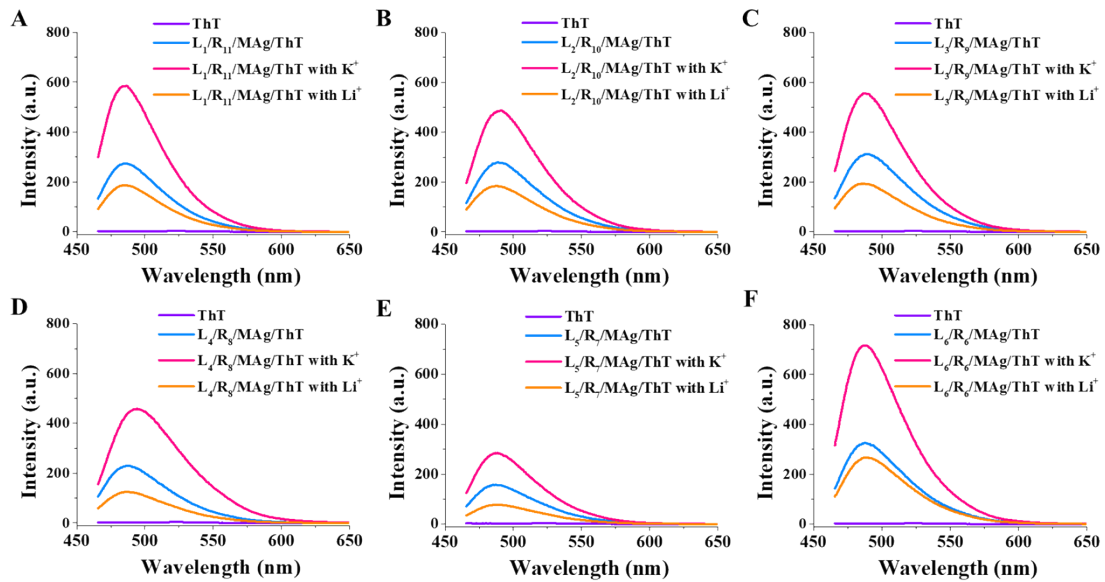


Fig. S4 Fluorescence spectra of ThT in PB buffer (purple line), ThT + three-element system in PB buffer (blue line), ThT + three-element system + K^+ in PB buffer (red line), ThT + three-element system + Li^+ in PB buffer (orange line), (A) $L_1/R_{11}/MAg$, (B) $L_2/R_{10}/MAg$, (C) $L_3/R_9/MAg$, (D) $L_4/R_8/MAg$, (E) $L_5/R_7/MAg$ and (F) $L_6/R_6/MAg$. The final concentrations of ThT, L_x , R_y , MAg, K^+ and Li^+ in PB buffer (20 mM, pH = 7.0, containing about 32 mM Na^+) were 2 μ M, 1 μ M, 1 μ M, 1 μ M, 100 mM and 100 mM, respectively.

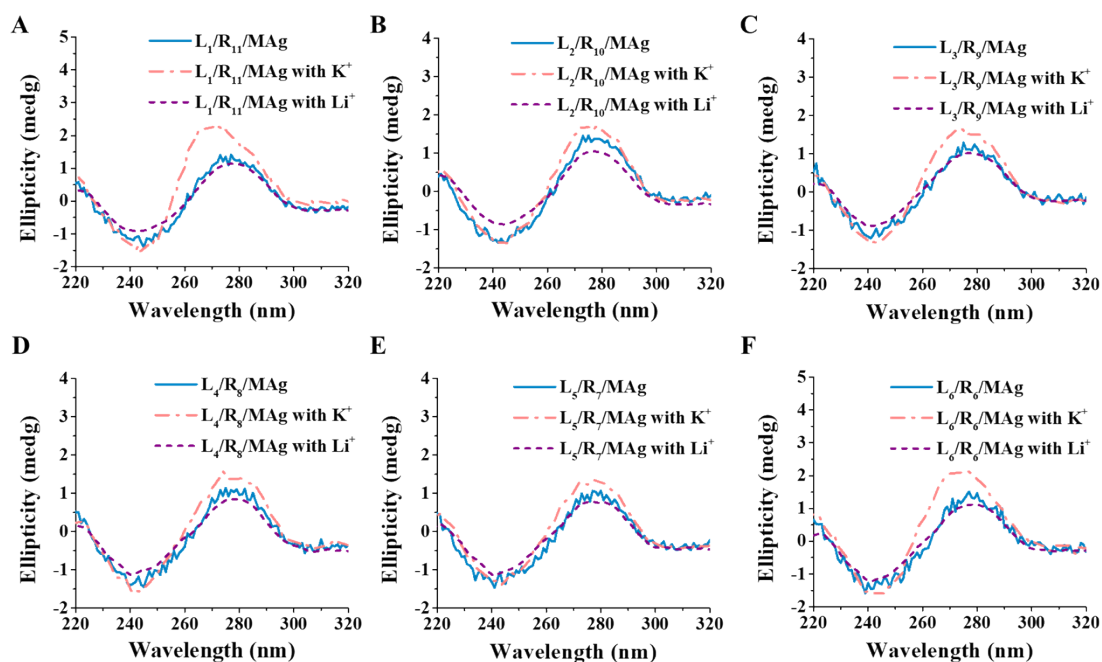


Fig. S5 Circular dichroism (CD) spectra of three-element system in PB buffer (blue curve), three-element system + K^+ in PB buffer (red dashed curve), three-element system + Li^+ in PB buffer (purple dashed curve), (A) $L_1/R_{11}/MAG$, (B) $L_2/R_{10}/MAG$, (C) $L_3/R_9/MAG$, (D) $L_4/R_8/MAG$, (E) $L_5/R_7/MAG$ and (F) $L_6/R_6/MAG$. The final concentrations of L_x , R_y , MAG , K^+ and Li^+ in PB buffer (20 mM, pH = 7.0, containing about 32 mM Na^+) were 2 μM , 2 μM , 2 μM , 100 mM and 100 mM, respectively.

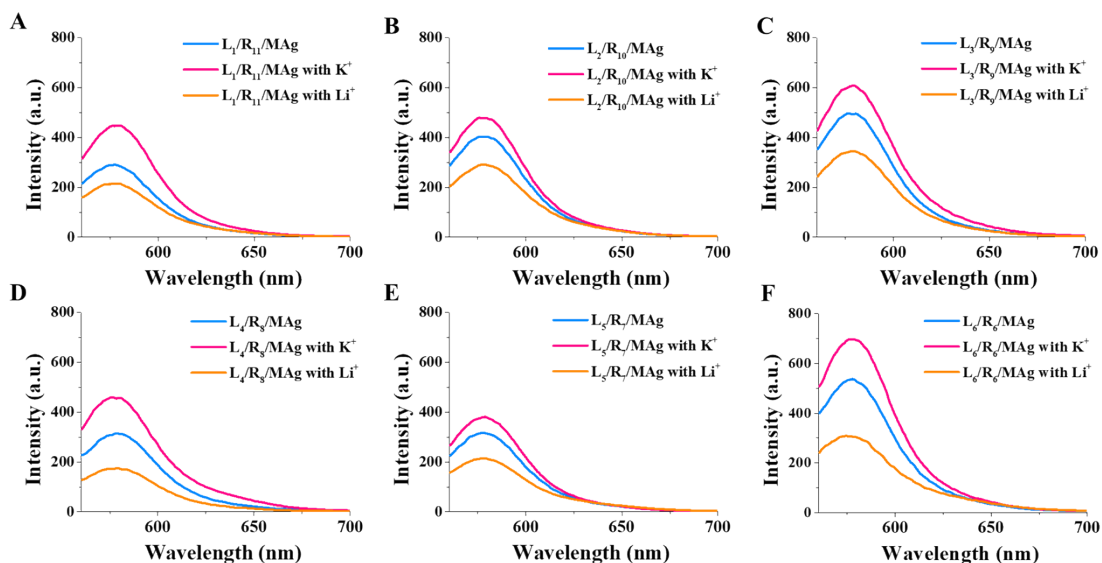


Fig. S6 The fluorescent spectra of AgNCs templated by $L_x/R_y/MAG$ in PB buffer (blue line), $L_x/R_y/MAG + K^+$ (red line), $L_x/R_y/MAG + Li^+$ (orange line). (A) $L_1/R_{11}/MAG$, (B) $L_2/R_{10}/MAG$, (C) $L_3/R_9/MAG$, (D) $L_4/R_8/MAG$, (E) $L_5/R_7/MAG$ and (F) $L_6/R_6/MAG$. The final concentrations of L_x , R_y , MAG , K^+ and Li^+ in PB buffer (20 mM, pH = 7.0, containing about 32 mM Na^+) were 1 μM , 1 μM , 1 μM , 100 mM and 100 mM, respectively.

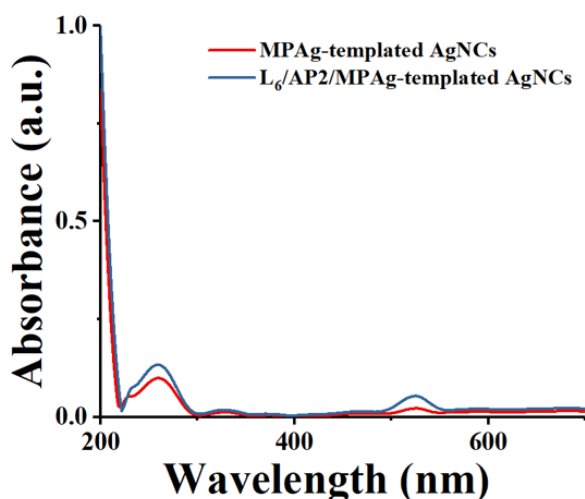


Fig. S7 UV absorption of AgNCs under different conditions.

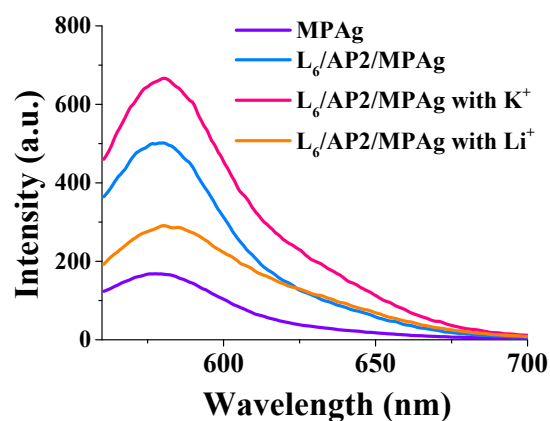


Fig. S8 The fluorescent spectra of AgNCs templated by MPAg (purple line), L₆/AP2/MPAg (blue line), L₆/AP2/MPAg + K⁺ (red line), L₆/AP2/MPAg + Li⁺ (orange line). The final concentrations of L₆, AP2, MPAg, K⁺ and Li⁺ in PB buffer (20 mM, pH = 7.0, containing about 32 mM Na⁺) were 1 μM, 1 μM, 1 μM, 100 mM and 100 mM, respectively.

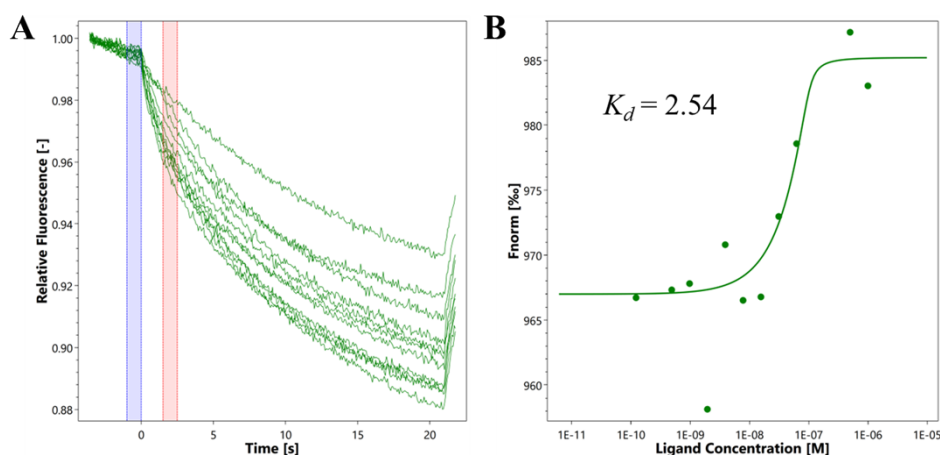


Fig. S9 The MST testing result between OME with AP2. (A) The trend line between time with relative fluorescence, (B) The fitted line between OME concentrations with the fluorescence ratio signal F_{norm} .

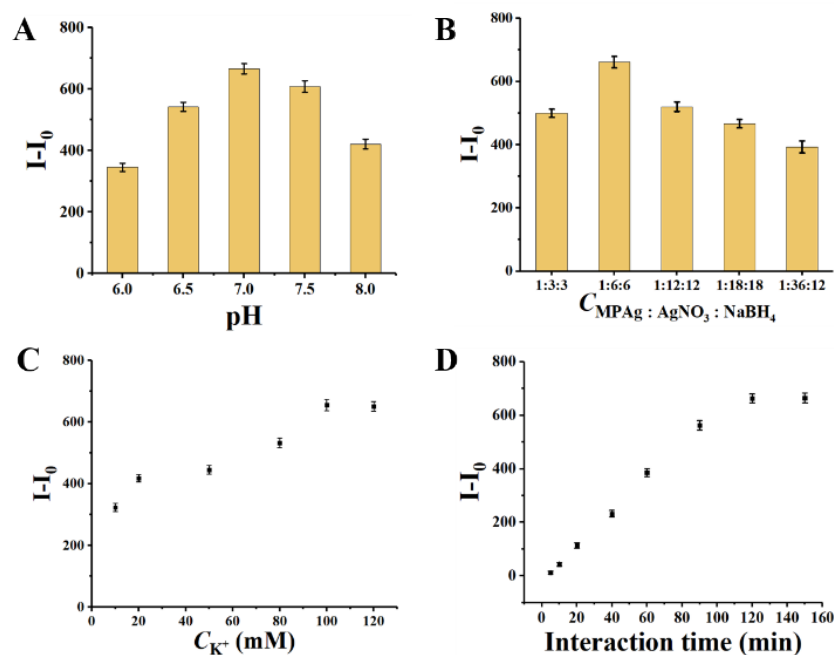


Fig. S10 Optimization results of different factors in this assay. (A) the fluorescence intensity responds to the pH values (6.0, 6.5, 7.0, 7.5, 8.0), (B) the fluorescence intensity responds to the concentration ratios of MPAG : Ag⁺ : NaBH₄ (1:3:3, 1:6:6, 1:12:12, 1:18:18, 1:36:18), (C) the fluorescence intensity responds to the concentration (10, 25, 50, 80, 100 and 120 mM) of K⁺, (D) the interaction time (5, 10, 20, 40, 60, 90, 120 and 150 min) of split G4 with MPAG-templated AgNCs.

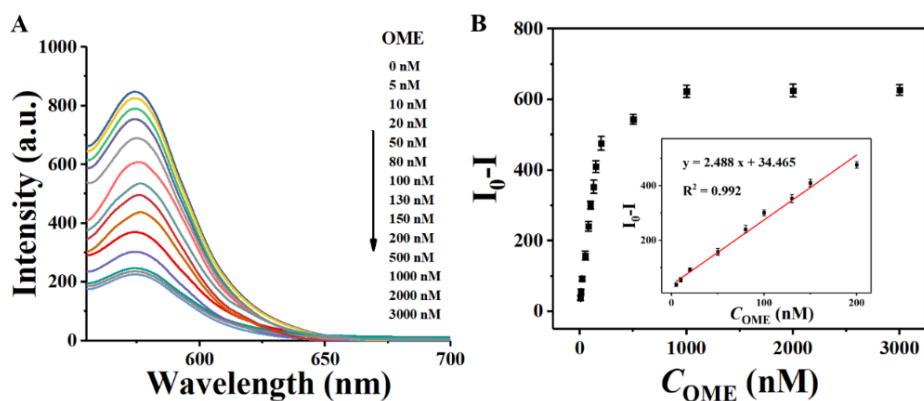


Fig. S11 (A) Fluorescent responses of this detection platform towards various concentrations of OME (0, 5, 10, 20, 50, 80, 100, 130, 150, 200, 500, 1000, 2000 and 3000 nM) in diluted Chinese cabbage extract (B) Relationship between relative fluorescence intensity and OME concentration in diluted Chinese cabbage extract; Inset shows the linear relationship between relative fluorescence intensity and OME concentration in diluted Chinese cabbage extract.

Reference

1. S. Wang, S. Lu, J. Zhao and X. Yang, *ACS Appl. Mater. Interfaces*, 2019, **11**, 25066-25073.
2. J. Xu and C. Wei, *Biosens. Bioelectron.*, 2017, **87**, 422-427.
3. J. Zhu, L. Zhang, S. Dong and E. Wang, *Chem. Sci.*, 2015, **6**, 4822-4827.
4. Y. Zhao, Y. Wang, R. Yang, H. Zhang, Y. Zhao, X. Miao and L. Lu, *Sens. Actuators. B Chem.*, 2021, **343**, 130172.
5. P. Wang, Y. Wan, A. Ali, S. Deng, Y. Su, C. Fan and S. Yang, *Sci. China Chem.*, 2016, **59**, 237-242.
6. R. V. Nair, P. R. Chandran, A. P. Mohamed and S. Pillai, *Anal. Chim. Acta*, 2021, **1181**, 338893.
7. T. Tang, J. Deng, M. Zhang, G. Shi and T. Zhou, *Talanta*, 2016, **146**, 55-61.
8. S. Ge, P. Zhao, M. Yan, D. Zang and J. Yu, *Anal. Methods*, 2012, **4**, 3150-3156.
9. Q. Zhang, Y. Yu, X. Yun, B. Luo, H. Jiang, C. Chen, S. Wang and D. Min, *ACS Appl. Nano Mater.*, 2020, **3**, 5212-5219.
10. C. Zhang, L. Wang, Z. Tu, X. Sun, Q. He, Z. Lei, C. Xu, Y. Liu, X. Zhang, J. Yang, X. Liu and Y. Xu, *Biosens. Bioelectron.*, 2014, **55**, 216-219.
11. S. Pang, T. P. Labuza and L. He, *Analyst*, 2014, **139**, 1895-1901.
12. X. Dou, X. Chu, W. Kong, J. Luo and M. Yang, *Anal. Chim. Acta*, 2015, **891**, 291-297.
13. S. Huang, M. Guo, J. Tan, Y. Geng, J. Wu, Y. Tang, C. Su, C. C. Lin and Y. Liang, *ACS Appl. Mater. Interfaces*, 2018, **10**, 39056-39063.
14. Y. Zhao, X. Li, J. Chen, X. Lu, Y. Yang, D. Song and F. Gao, *Sens. Actuators B Chem.*, 2022, **352**, 131072.
15. L. Huang, D.-W. Sun, H. Pu, Q. Wei, L. Luo and J. Wang, *Sens. Actuators B Chem.*, 2019, **290**, 573-580.
16. G. Song, J. Zhang, H. Huang, X. Wang, X. He, Y. Luo, J.-c. Li, K. Huang and N. Cheng, *Food Chem.*, 2022, **387**, 132896.
17. X. Zhao, W. Kong, J. Wei and M. Yang, *Food Chem.*, 2014, **162**, 270-276.
18. R. Raposo, M. Barroso, S. Fonseca, S. Costa, J. A. Queiroz, E. Gallardo and M. Dias, *Rapid Commun. Mass Sp.*, 2010, **24**, 3187-3194.
19. X. Liu, M. Song, T. Hou and F. Li, *ACS Sensors*, 2017, **2**, 562-568.
20. M. A. Montesano, A. O. Olsson, P. Kuklennyik, L. L. Needham, A. S. A. Bradman and D. B. Barr, *J. Expo. Sci. Env. Epid.*, 2007, **17**, 321-330.
21. Y. Zhao, Y. Wang, R. Yang, H. Zhang, Y. Zhao, X. Miao and L. Lu, *Sens. Actuators B Chem.*, 2021, **343**, 130172.